Electronic Supplementary Material (ESI) for Soft Matter.

Supporting Information

Effect of Surface Modification on Interfacial Nanobubble Morphology and Contact Line Tension

Kaushik K. Rangharajan, Kwang J. Kwak, A.T. Conlisk, Yan Wu* & Shaurya Prakash*

Corresponding authors

*Shaurya Prakash; **E-mail:** prakash.31@osu.edu, *Yan Wu; **E-mail:** wuy@uwplatt.edu

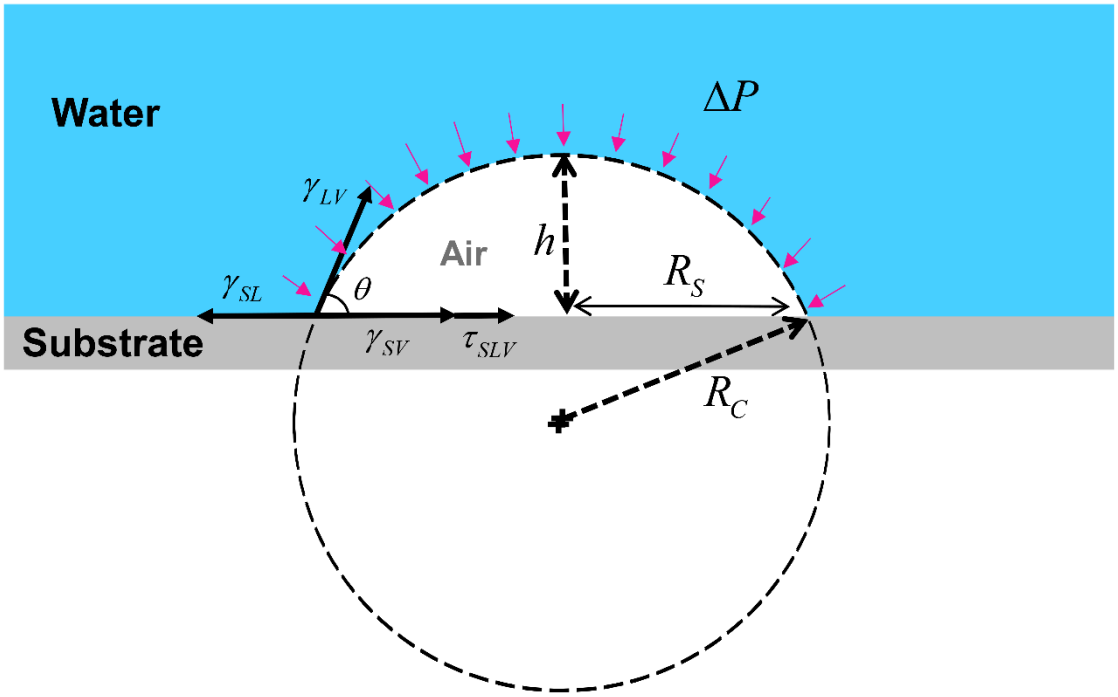

Figure S1. Free body diagram of a nanobubble pinned to a substrate surrounded by water, where h is the nanobubble height, R_s is the nanobubble lateral radius, R_c is the radius of curvature, ΔP is the Laplace pressure, and τ_{SLV} is three phase contact line tension. $\gamma_{LV}, \gamma_{SL}, \gamma_{SV}$ are the liquid-vapor, solid-liquid, and solid-vapor surface tensions respectively. The geometric dimensions used in this figure arise from tip-corrected AFM measurements as described in the main manuscript.

Vertical force balance to estimate Laplace pressure

$$(\gamma_{LV}\, Sin\theta)\, 2\pi R_s - \Delta P\, \pi\, R_s^{\,2} = 0$$

$$\Delta P = \frac{2\gamma_{LV}\, Sin\theta}{R_s}$$

$$\frac{R_s}{Sin\theta} = R_c$$

$$\Delta P = \frac{2\gamma_{LV}}{R_c} (Laplace\ pressure)$$

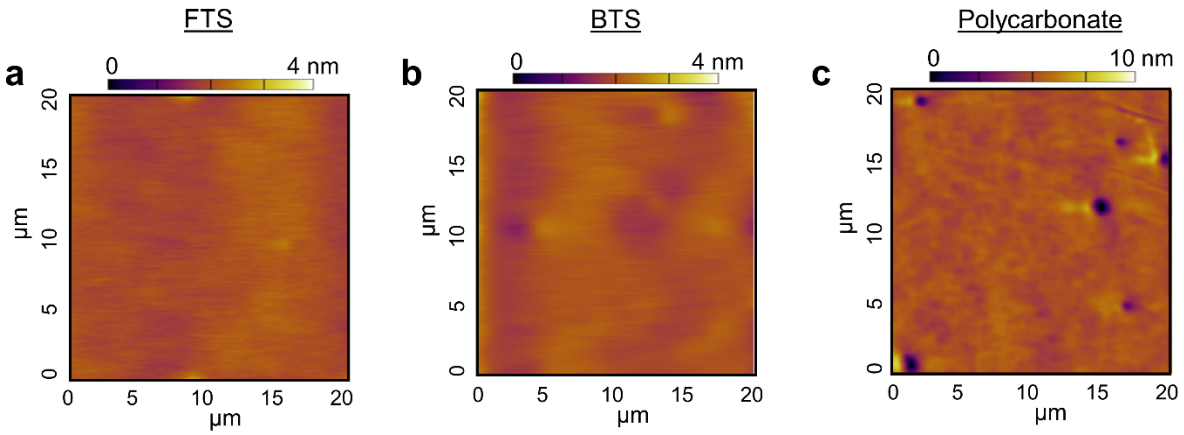

Figure S2. TM-AFM scans in air showing roughness plot for a) FTS b) BTS and c) Polycarbonate over a scan area of 20 µm x 20 µm. The RMS roughness values are described in Table 1 in the main manuscript.

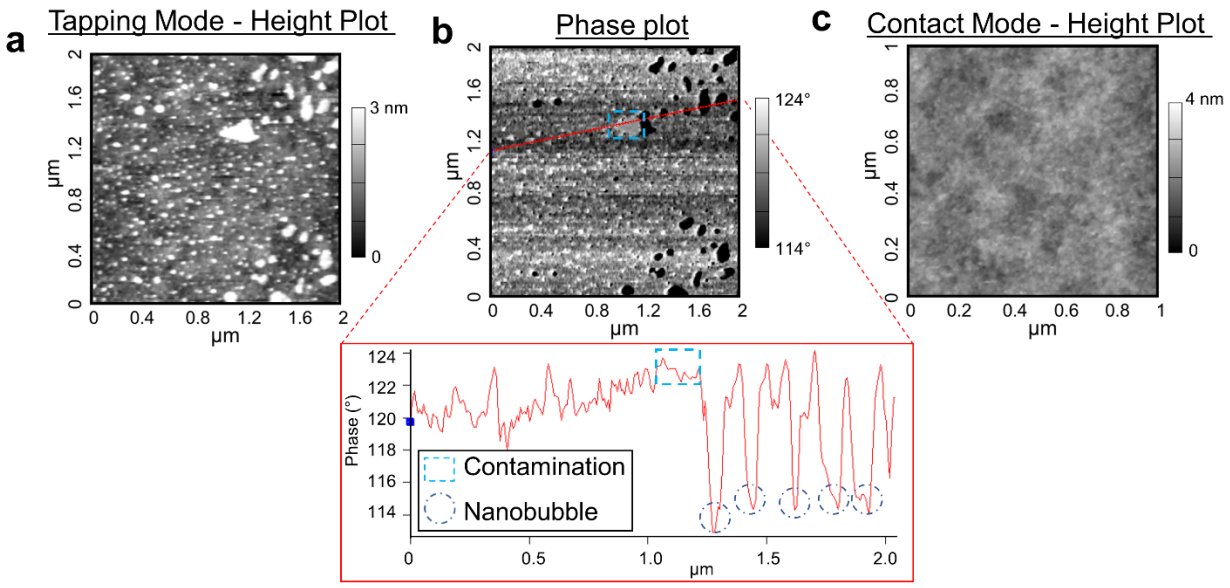

Figure S3: Figure S3.a) 2 µm x 2 µm tapping mode scan of polycarbonate immersed in air-equilibrated water. b) Corresponding phase plot that shows a phase shift of ~8° over nanobubbles, which is significantly higher in comparison to the phase shift over the contamination (~0.5° phase shift). The phase plot also clearly shows that the scanning was done in the attractive regime as phase > 90° c) Hard contact mode scan of polycarbonate substrate in air-equilibrated water does not show any nanobubbles.

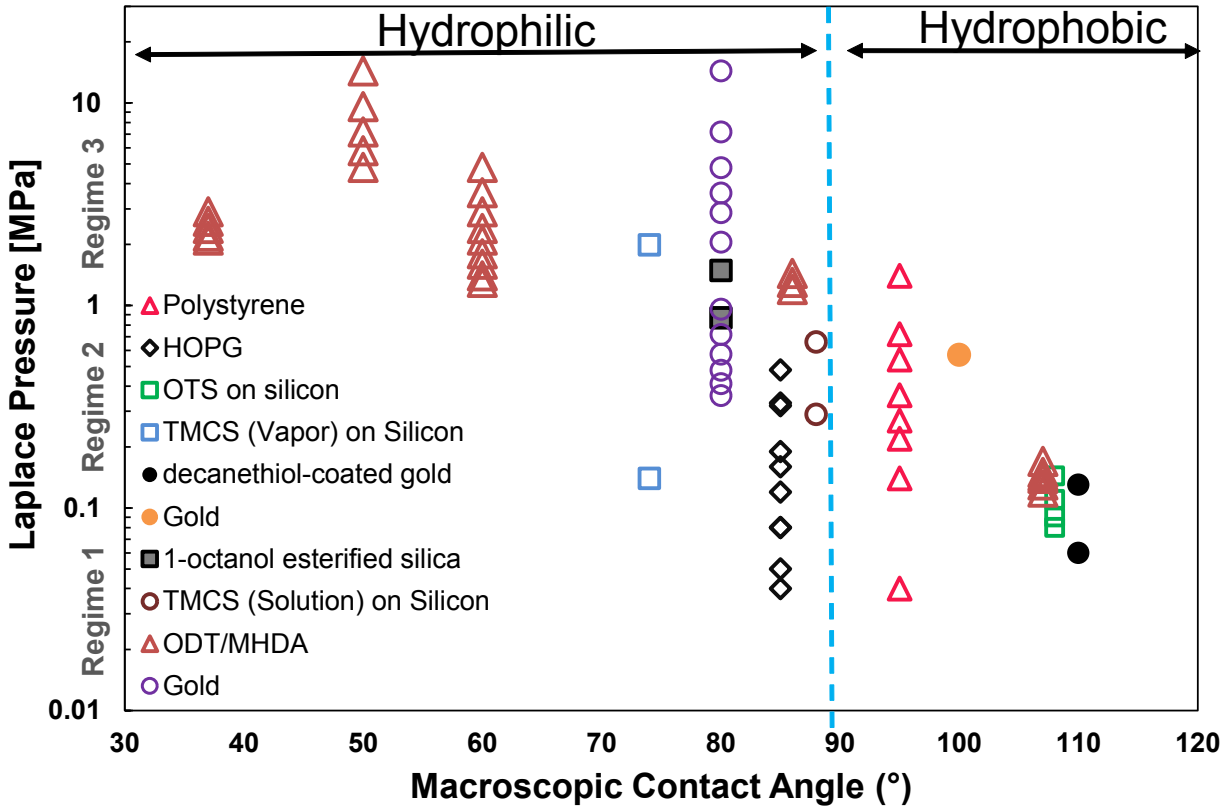

Figure S4. Regime map summarizing Laplace pressure variation of surface nanobubbles as a function of macroscopic contact angle. Except for HOPG (◊), where most nanobubbles were introduced via solvent exchange, all hydrophilic substrates sustain nanobubbles of Laplace pressure that is higher than atmospheric pressure by an order of magnitude (regime 3). Polystyrene (Δ)(Contact angle 94° - 96°) has nanobubbles spread across regime 2 and as the surfaces become progressively hydrophobic, the Laplace pressure distribution is primarily limited to regime 1 and lower levels of regime 2. Nanobubbles formed on hydrophilic gold (○) belong to regime 3 when imaged in air-equilibrated water and drop down to regime 2 when imaged in 25% ethanol-water mixture. Importantly, the range of observed Laplace pressures for similar conditions, including similar surface chemistry, points to the fact that nanobubble size and stability hypotheses cannot yet be generalized. Figure S2 shows a broad summary of Laplace pressures indicating sizes of nanobubbles for a variety of reported substrates. It is worth noting that even for similar substrates, no consensus exists on size and therefore subsequent Laplace pressure for the nanobubble observations suggesting that a variety of experimental conditions affect formation, size, and eventual stability of nanobubbles.

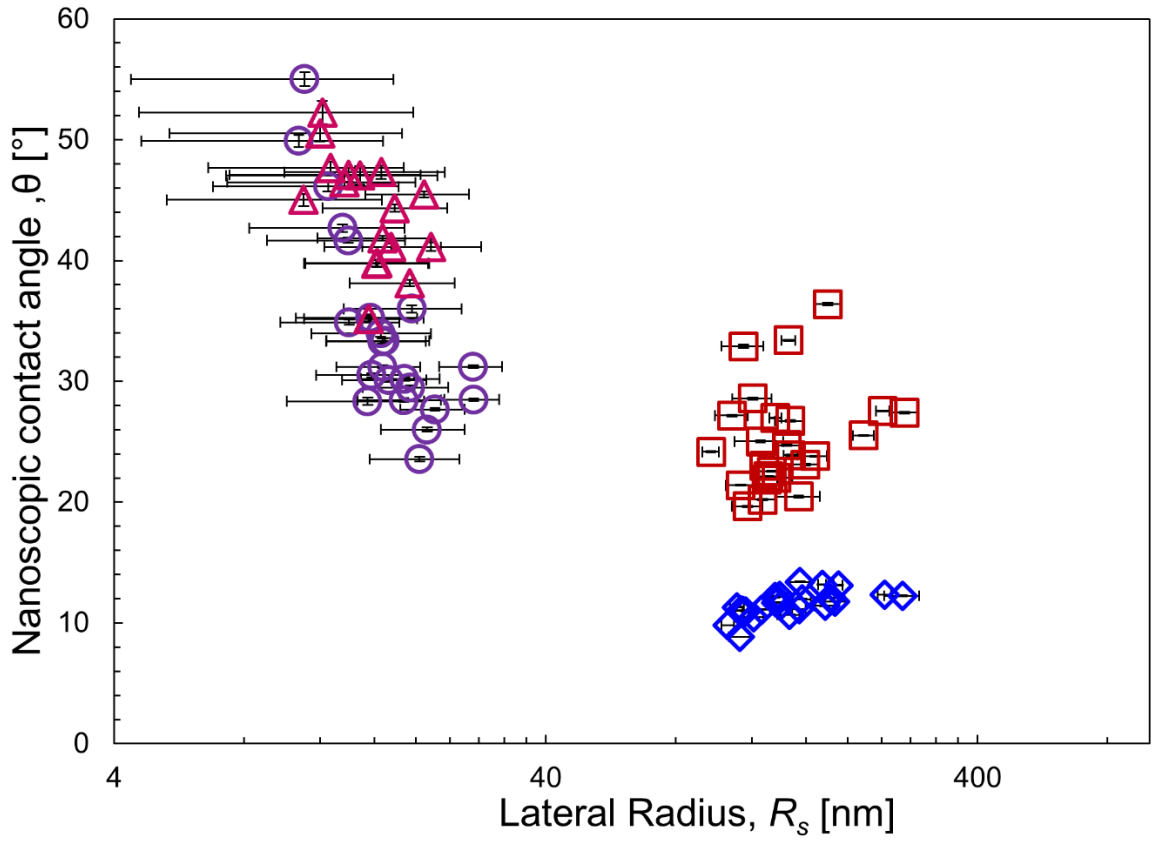

Figure S5. Plot of nanoscopic contact angle, θ compared with lateral radius, R_s for nanobubbles formed on fluoro-terminated silica (FTS, □), bromo-terminated silica (BTS, O), polycarbonate imaged with air-equilibrated water (Δ) and polycarbonate imaged after ethanol exchange method (◊). The nanoscopic contact angle varies as 25.2° ± 4.2° for FTS, 34.2° ± 7.9° for BTS, 44.1° ± 4.5° for polycarbonate imaged with air-equilibrated water and 11.5° ± 1.0° for polycarbonate imaged after ethanol exchange method. Also, nanobubbles with R_s< 50 nm on an average have a higher θ compared to those with R_s> 50 nm. Moreover, the nanoscopic contact angle for all the bubbles is significantly smaller compared to the macroscopic contact angle of a substrate measured via sessile drop method. Previous study by Borkent et al.[†] also provides a literature summary of the value of θ over several substrates such as HOPG, Si – OTS, Polystyrene, Gold etc. but not the substrates analyzed in the present study. Also, the effect of ethanol exchange on changes to nanobubble morphology is not taken into account. In the present study, it is observed that the lateral radius of polycarbonate increases by an order of magnitude after ethanol exchange and the nanoscopic contact angle decreases by 32.6°. Error bars indicate one standard deviation of representative parameters.

[†] B.M. Borkent, S. de Beer, F. Mugele, D. Lohse, *Langmuir* 2009, **26**(1):260-268

Table S1. Reference information for various data points used in plotting the regime map.

Substrate (contact angle °)	**Laplace Pressure [MPa]**	**Supersaturated**	**Reference**
Regime 1			
Polystyrene on Silicon (94 - 96)	0.04	No	S1
HOPG (NA)	0.05	Solvent exchange	S2
HOPG (NA)	0.04	Solvent exchange	S2
OTS silicon (108)	0.08	Solvent exchange	S3
HOPG (NA)	0.08	Solvent exchange	S4
decanethiol-coated gold(Adv 110°)	0.06	Solvent exchange	S5
OTS on silicon (Adv 112°)	0.09	Solvent exchange	S6
Regime 2			
OTS on silicon (Adv 112°)	0.14	Solvent exchange	S6
Polystyrene on Silicon (94 - 96)	0.14	No	S1
TMCS Vapor on Silicon (Adv 74°)	0.14	Using CO_2	S7
TMCS Solution on Silicon (Adv 88°)	0.29	Using CO_2	S1
TMCS Solution on Silicon (Adv 88°)	0.66	Using CO_2	S1
1-octanol esterified silica (Adv 80°)	0.87	Solvent exchange	S8
HOPG (NA)	0.16	Solvent exchange	S9
Gold (100°)	0.57	No	S10
Polystyrene (97)	0.27	No	S11
Polystyrene (NA)	0.72	No	S12
Polystyrene (NA)	0.22	No	S12
HOPG (NA)	0.32	Solvent exchange	S13
HOPG (NA)	0.12	Solvent exchange	S13
HOPG (NA)	0.33	No	S14
HOPG (NA)	0.19	Solvent exchange	S15
decanethiol-coated gold (Adv 110°)	0.13	Solvent exchange	S5
OTS on silicon (110°)	0.11	No	S16
ODT/MHDA (107°)	0.17,0.15,0.144 0.14,0.13,0.12	No	S17
Polystyrene on Silicon (95 °)	0.54	No	S18

Polystyrene on Silicon (95 °)	0.36	No	S18
Gold (80°)	0.96,0.72,0.58, 0.48,0.41,0.36	Solvent exchange	S19
Regime 3			
1-octanol esterified silica (80 Adv)	1.49	Solvent exchange	S8
Polystyrene - film (95)	1.4	No	S20
TMCS Vapor on Silicon (Adv 74°)	1.99	Using CO_2	S1
ODT/MHDA (86°)	1.2,1.31,1.44	No	S17
ODT/MHDA (60°)	4.8,3.6,2.9,2.4,2.1, 1.8,1.6,1.4,1.3	No	S17
ODT/MHDA (50°)	14.4, 9.6, 7.2, 5.8, 4.8	No	S17
ODT/MHDA (37°)	2.9, 2.6, 2.4, 2.2, 2.1	No	S17
Gold (80°)	14.4,7.2,4.8, 3.6,2.9,2.1	No	S19

Abbreviations

HOPG, Highly ordered pyrolytic graphite; ODT, octadecanethiol; OTS, Octadecyltrichlorosilane; MHDA, 16-mercaptohexadecanoic acid; TMCS, Trimethylchlorosilane;

References

S1. D. Li, D. Jing, Y. Pan, W. Wang and X. Zhao, *Langmuir*, 2014, **30**, 6079-6088.

S2. X. H. Zhang, X. Zhang, J. Sun, Z. Zhang, G. Li, H. Fang, X. Xiao, X. Zeng and J. Hu, *Langmuir*, 2006, **23**, 1778-1783.

S3. X. H. Zhang, N. Maeda and V. S. J. Craig, *Langmuir*, 2006, **22**, 5025-5035.

S4. M. A. Hampton and A. V. Nguyen, *Minerals Engineering*, 2009, **22**, 786-792.

S5. X. Zhang, D. Y. C. Chan, D. Wang and N. Maeda, *Langmuir*, 2013, **29**, 1017-1023.

S6. X. H. Zhang, A. Quinn and W. A. Ducker, *Langmuir*, 2008, **24**, 4756-4764.

S7. J. Yang, J. Duan, D. Fornasiero and J. Ralston, *The Journal of Physical Chemistry B*, 2003, **107**, 6139-6147.

S8. M. A. Hampton and A. V. Nguyen, *Advances in Colloid and Interface Science*, 2010, **154**, 30-55.

S9. Y. Chih-Wen, L. Yi-Hsien and H. Ing-Shouh, *Journal of Physics: Condensed Matter*, 2013, **25**, 184010.
S10. M. Holmberg, A. Kühle, K. A. Mørch and A. Boisen, *Langmuir*, 2003, **19**, 10510-10513.
S11. A. Agrawal, J. Park, D. Y. Ryu, P. T. Hammond, T. P. Russell and G. H. McKinley, *Nano Letters*, 2005, **5**, 1751-1756.
S12. A. C. Simonsen, P. L. Hansen and B. Klösgen, *Journal of Colloid and Interface Science*, 2004, **273**, 291-299.
S13. B. Zhao, Y. Song, S. Wang, B. Dai, L. Zhang, Y. Dong, J. Lu and J. Hu, *Soft Matter*, 2013, **9**, 8837-8843.
S14. R. P. Berkelaar, H. J. W. Zandvliet and D. Lohse, *Langmuir*, 2013, **29**, 11337-11343.
S15. W. Shuo, L. Minghuan and D. Yaming, *Journal of Physics: Condensed Matter*, 2013, **25**, 184007.
S16. N. Ishida, T. Inoue, M. Miyahara and K. Higashitani, *Langmuir*, 2000, **16**, 6377-6380.
S17. B. Song, W. Walczyk and H. Schönherr, *Langmuir*, 2011, **27**, 8223-8232.
S18. B. Bhushan, Y. Wang, A. Maali, *Journal of Physics: Condensed Matter*, 2008, **20**, 485004.
S19. N. Kameda and S. Nakabayashi, *Chemical Physics Letters*, 2008, **461**, 122-126.
S20. Y. Wang, B. Bhushan and X. Zhao, *Langmuir*, 2009, **25**, 9328-9336.